Available online at www.sciencedirect.com
ScienceDirect
Physica A 370 (2006) 390–406
PHYSICA A
www.elsevier.com/locate/physa

Phase transitions in small systems: Microcanonical vs. canonical ensembles

Jörn Dunkel[a,*], Stefan Hilbert[b]

[a]Institute for Physics, Universität Augsburg, Universitätsstraße 1, D-86135 Augsburg, Germany
[b]Institute for Physics, Humboldt-Universität zu Berlin, Newton-Straße 15, D-12489 Berlin, Germany

Received 4 December 2005; received in revised form 15 February 2006
Available online 6 June 2006

Abstract

We compare phase transition(-like) phenomena in small model systems for both microcanonical and canonical ensembles. The model systems correspond to a few classical (non-quantum) point particles confined in a one-dimensional box and interacting via Lennard-Jones-type pair potentials. By means of these simple examples it can be shown already that the microcanonical thermodynamic functions of a small system may exhibit rich oscillatory behavior and, in particular, singularities (non-analyticities) separating different microscopic phases. These microscopic phases may be identified as different microphysical dissociation states of the small system. The microscopic oscillations of microcanonical thermodynamic quantities (e.g., temperature, heat capacity, or pressure) should in principle be observable in suitably designed evaporation/dissociation experiments (which must realize the physical preconditions of the microcanonical ensemble). By contrast, singular phase transitions cannot occur, if a small system is embedded into an infinite heat bath (thermostat), corresponding to the canonical ensemble. For the simple model systems under consideration, it is nevertheless possible to identify a smooth canonical phase transition by studying the distribution of complex zeros of the canonical partition function.

Keywords: Microscopic phase transitions; Small systems; Lennard-Jones chains

1. Introduction

One of the most intriguing thermodynamic properties of various macroscopic systems is their ability to undergo phase transitions (PTs) if one or more control parameters pass certain critical values [1,2]. The first systematic classification scheme for macroscopic PTs was proposed by Ehrenfest and Ehrenfest [3] in 1912 already. After further pioneering work by Mayer et al. [4–7], Yang and Lee [8,9] elucidated the mathematical essence underlying PTs in the *grandcanonical* ensemble by studying the distribution of complex zeros (DOZs) of the grandcanonical partition function. Later on, Fisher [10] and Grossmann et al. [11–13] employed a very similar approach to analyze the temperature dependence of PTs in the *canonical* ensemble (CE). Recently,

*Corresponding author. Tel.: +49 821 5983229; fax: +49 821 5983222.
E-mail addresses: joern.dunkel@physik.uni-augsburg.de, dunkel@mpa-garching.mpg.de (J. Dunkel).
URL: http://www.physik.uni-augsburg.de/~dunkeljo.

0378-4371/$ - see front matter © 2006 Elsevier B.V. All rights reserved.
doi:10.1016/j.physa.2006.05.018

further significant progress in the understanding of critical phenomena has been achieved by studying the connection between PTs and phase (or configuration) space topology [14–20].

Formally, the seminal contributions [3–13] have in common that, in the spirit of traditional thermodynamics, they refer to macroscopically large systems; more exactly, to systems satisfying the thermodynamic limit (corresponding to $N, V, E \to \infty$ such that number density $n = N/V$ and energy density $e = E/N$ remain constant). However, the rapid experimental and computational progress during the last two decades led to an increasing interest in extending thermodynamic concepts to 'small' systems, containing—by definition—only a very limited number of DOF [21–25]. Experiments on finite systems include, e.g., investigations of two-dimensional Coulomb clusters in dusty plasmas [26,27], Bose–Einstein condensation in magneto-optical traps [28,29], and transitions in sodium clusters [30]. These experimental investigations were accompanied by extensive theoretical and numerical studies (see, e.g., Refs. [31–33]).

Simultaneously, interest began to focus on the question how to identify and classify the finite-size analogs of macroscopic PTs. Important results in this regard were obtained by Wales et al. [23,24], who considered necessary and sufficient criteria for phase coexistence in finite systems. A general classification scheme for smooth canonical PTs in small systems was proposed by Borrmann et al. [34]. Pursuing an approach similar to that of Yang and Lee [8,9], Fisher [10] and Grossmann et al. [11–13], these authors suggest to use the DOZ in order to characterize transitions in the CE of small systems (cf. Section 3.2). Mülken et al. [35] and Alves et al. [36] compare the DOZ classification scheme with alternative proposals made by Gross [25,37] and by Janke and Kenna [38], respectively.

Such progress notwithstanding, there still exist some open questions regarding which types of non-analytic PTs can occur in small systems. For (*grand-*)*canonical* ensembles, it is well established that truly singular PTs can be observed in the thermodynamic limit only, corresponding to a system with formally infinite particle number $N \to \infty$ [8–13,34,39]. In contrast to this, the microcanonical thermodynamic functions (TDFs) may exhibit non-analytic behavior even at finite N. For example, recently, Pleimling and Behringer [40] have found singularities in microcanonical quantities of finite three-dimensional spin models, which announce a continuous *macroscopic* PT of the infinite systems. Additionally, as we intend to demonstrate here by means of very simple examples, the microcanonical TDFs of a small system can also exhibit non-analytic *microscopic* PTs,[1] characterized by well-defined critical energy values and typically accompanied by strong variations of thermodynamic observables (e.g., oscillations of temperature, heat capacity and pressure). From the physical point of view, such microscopic PTs correspond to transitions between different dissociation states of the system. Hence, they are important indicators for essential structural changes in the small system under consideration (quite analogous to singular points indicating macroscopic PTs). For reasons of simplicity, the discussion in the present paper will be restricted to one-dimensional (1D) models, but the general mechanism responsible for the singular and oscillatory behavior of microcanonical thermodynamic observables works analogously in two and three spatial dimensions. Hence, it should in principle be possible to observe such microscopic oscillations in suitably designed evaporation/dissociation experiments (which must, of course, realize the physical preconditions of the microcanonical ensemble (MCE)).

The paper is organized as follows: Section 2 is dedicated to microscopic PTs in the MCE of small model systems. As examples, we will consider isolated 1D chains with Lennard-Jones (LJ) pair interactions and also the Takahashi gas [44]. It will be shown that these simple systems exhibit singular microscopic PTs, separating different microcanonical dissociation states. Subsequently, the Takahashi gas will be used in Section 3 to investigate the relation between singular microscopic PTs in the MCE and smooth PTs in the CE as defined by the DOZ scheme [34]. The paper concludes with a summary of the main results in Section 4.

2. Microscopic PTs in the MCE

Classical microcanonical thermodynamics refers to an ensemble of thermally isolated systems, completely described by their Hamiltonian dynamics. Due to the fact that the systems are decoupled from the

[1]The appearance of such microcanonical singular points even in the 1D case is *not* in conflict with van Hove's theorem for the canonical ensemble [41,42], since for most small systems (as well as for many 'large' systems) the microcanonical and canonical ensembles are generally *not* equivalent (see, e.g. Ref. [43]).

environment, the energy E is a conserved quantity, i.e., there are no energy fluctuations in the MCE. In particular, as will be demonstrated in Sections 2.3 and 2.4, the microcanonical TDFs may exhibit singular points even in the case of small systems.

2.1. The microcanonical ensemble

For the sake of simplicity we will confine ourselves to examples, where the thermodynamic state is completely characterized by two control parameters, namely, energy E and volume number V (generalizations to problems with additional macroscopic variables, e.g., the strength of external magnetic fields, are straightforward). More precisely, we will consider N identical point-like particles of mass m, moving in D equivalent spatial dimensions; i.e., the number of degree of freedom (DOF) reads $d = DN$ and the volume is given by $V = L^D$, where L is the length of the confining cube (volume interval). The deterministic dynamics of the system is assumed to be governed by a Hamiltonian of the standard form

$$H(q,p;V) = K(p) + U(q;V) = E, \tag{1a}$$

where $q = (q_1,\ldots,q_d)$ and $p = (p_1,\ldots,p_d)$ are generalized coordinates and momenta, respectively. The kinetic energy K and the potential energy U are given by

$$K(p) = \sum_{i=1}^{d} \frac{p_i^2}{2m}, \quad U(q;V) = U_{\text{pair}}(q) + U_{\text{box}}(q;V), \tag{1b}$$

where $U_{\text{pair}}(q)$ represents the pair interactions of the particles, and the box potential is defined by

$$U_{\text{box}}(q;V) = \begin{cases} 0, & q \in [-L/2, L/2]^N, \\ +\infty & \text{otherwise.} \end{cases} \tag{1c}$$

The primary thermodynamic potential of the MCE is the entropy $S = S(E,V)$, which is related to the microcanonical 'partition' function $\mathscr{Z}_{\text{M}}(E,V)$ by [45]

$$S = k \ln \mathscr{Z}_{\text{M}}, \tag{2}$$

with k denoting the Boltzmann constant. The equations of state (EOS) for the temperature T and pressure P are obtained by [25,45–49]

$$\frac{1}{T} \equiv \frac{\partial S}{\partial E}, \quad \frac{P}{T} \equiv \frac{\partial S}{\partial V}. \tag{3}$$

That is, the temperature T of the MCE is a derived quantity, which is in contrast to the CE (see Section 3.1), where the temperature is one of the adjustable external control parameters.

During the past century, various different definitions for the microcanonical partition function $\mathscr{Z}_{\text{M}}$, or the entropy S, have been proposed and investigated. For classical systems as described by the Hamiltonian function (1a), the two most commonly used definitions for $\mathscr{Z}_{\text{M}}(E,V)$ read [25,45–49]

$$\mathscr{Z}_{\text{M}} = \Omega, \tag{4a}$$

$$\mathscr{Z}_{\text{M}} = \varepsilon_0 \frac{\partial \Omega}{\partial E}, \tag{4b}$$

where the phase volume Ω is given by (h denotes the Planck constant)

$$\Omega(E,V) \equiv \frac{1}{N! h^d} \int_{\mathbb{R}^d} \mathrm{d}q \int_{\mathbb{R}^d} \mathrm{d}p\, \Theta(E - H(q,p;V)). \tag{5}$$

The Heaviside unit step function $\Theta(x)$, appearing in Eq. (5), is defined by $\Theta(x) = 0$ for $x < 0$ and $\Theta(x) = 1$ for $x \geqslant 0$. The additional parameter ε_0 in Eq. (4b) is a small energy constant that quantifies the thickness of a thin energy shell around the phase space surface defined by $H(q,p,V) = E$ and is formally required to make $\mathscr{Z}_{\text{M}}$ dimensionless.

It is well-known that the definitions (4a) and (4b) may yield (almost) identical results [39,45,47,48] in the thermodynamic limit, i.e., if N is large. However, for small systems they lead to essentially different TDFs. To briefly illustrate this, let us consider an ideal gas with N non-interacting particles, moving in the D-dimensional volume V. In this case, the phase volume is given by [45]

$$\Omega(E,V)=\frac{(\pi 2mE)^{d/2}}{N!h^d\Gamma(d/2+1)}V^N, \tag{6}$$

where $\Gamma(x)$ is Euler's Gamma-function. Definition (4a) then yields the EOS

$$E=\frac{d}{2}kT, \quad \frac{P}{T}=\frac{kN}{V}, \tag{7}$$

whereas one obtains from definition (4b)

$$E=\left(\frac{d}{2}-1\right)kT, \quad \frac{P}{T}=\frac{kN}{V}. \tag{8}$$

For systems with $d\gg 1$ the difference in the energy equations is negligible, but for small systems it becomes relevant. In particular, for $d=1$ Eq. (8) yields a negative temperature at positive energy. Obviously, a similarly unreasonable result is obtained for $d=2$. This indicates that the partition function (4b) is inappropriate for systems with low-dimensional phase space.

More generally speaking, only Eq. (4a) reproduces correctly the well-known laws of thermodynamics and also yields the correct equipartition theorem for an arbitrary number d of DOF, whereas the Eq. (4b) leads to inconsistencies if d is small. This important aspect was first realized by Hertz [50,51], and, later on, also emphasized by Becker [45], Berdichevsky and Alberti [52,53] and Adib [54]. In particular, denoting the ensemble average with respect to the microcanonical probability density function $f(q,p)\propto\delta(E-H(q,p))$ by $\langle\cdot\rangle_{\mathrm{MCE}}$, it can be shown [45,46] that the (equipartition) identity

$$\frac{kT}{2}=\frac{1}{d}\langle K(p)\rangle_{\mathrm{MCE}}=\left\langle\frac{p_i^2}{2m}\right\rangle_{\mathrm{MCE}} \quad \forall i=1,\ldots,d \tag{9}$$

holds, only if one employs the Hertz entropy definition

$$S\equiv k\ln\Omega. \tag{10}$$

Due to these reasons, all subsequent considerations will be based on Eq. (10).[2] For Hamiltonians as in Eq. (1a) one can still perform the momentum integration in Eq. (5) using d-dimensional spherical coordinates, yielding

$$\Omega(E,V)=\frac{O_d}{N!h^d d}\int_{\mathbb{R}^d}\mathrm{d}q\,\{2m[E-U(q;V)]\}^{d/2}\Theta(E-U(q;V)), \tag{11}$$

where $O_d=2\pi^{d/2}/\Gamma(d/2)$ denotes the surface of the d-dimensional unit sphere.

2.2. Macroscopic vs. microscopic PTs

Conventionally, *macroscopic* PTs are singularities (non-analyticities) of TDFs that arise in the thermodynamic limit, corresponding to an infinitely large system. The first systematic classification of macroscopic PTs goes back to Ehrenfest [3,55]. According to the Ehrenfest scheme, a PT is indicated by a non-analyticity of the Gibbs free enthalpy $G(T,P,\ldots)$, assumed to be a function of the temperature T, pressure P and other external control parameters. The order of the PT is determined by the lowest order at which any of the derivatives of $G(T,P,\ldots)$ becomes non-continuous. Since the Ehrenfest scheme has turned out to be too narrow in many cases, it is nowadays often preferred to merely distinguish *discontinuous* (*first-order*) and *continuous* (*second-order*) transitions.

Extending this concept to small systems, any non-analyticity of the thermodynamic potential as function of the external control parameters may be called a PT. However, to avoid ambiguities, we shall speak of

[2]This is e.g., in contrast to Refs. [25,35,37] where the Boltzmann definition (4b) is considered.

microscopic PTs when discussing singular (non-analytic) points in the microcanonical TDFs of small systems. Furthermore, we will adopt the following terminology to classify microscopic PTs in the MCE: If the primary thermodynamic potential, the Hertz entropy S, is discontinuous, then we will call the PT discontinuous; if S is non-analytic but continuous, the microscopic PT is called continuous.

Let us next discuss how the formal (Ehrenfest-type) order of a microscopic PT depends on the number of DOF. For systems described by Hamiltonian (1a), the phase volume (11) is related to the admissible configuration space volume

$$\omega(E,V)=\int_{\mathbb{R}^d} \mathrm{d}q\,\Theta(E-U(q;V)) \tag{12}$$

via[3]

$$\frac{\partial^{d/2}\Omega(E,V)}{\partial E^{d/2}}=\frac{(2\pi m)^{d/2}}{N!h^d}\omega(E,V). \tag{13}$$

If, at a given critical energy $E_c(V)$, $\omega(E,V)$ has continuous derivatives up to order j, but a discontinuous $(j+1)$st derivative, then $\Omega(E,V)$ and hence $S(E,V)$ have continuous derivatives up to order $(j+d/2)$, but a discontinuity in the $(j+d/2+1)$st derivative. Consequently, the formal order of the PT equals $(j+d/2+1)$, i.e., the order increases with an increasing number of DOF. For the examples discussed below, the differentiability class of the admissible configuration space volume $\omega(E,V)$ does not change with particle number ($j=0$ for LJ chains and $j=-1$ for the Takahashi gas), and we indeed observe such an increasing order with increasing particle number (cf. results of Section 2.3.2).[4]

2.3. Singular microscopic PTs in LJ chains

To demonstrate the appearance of non-analytic microscopic PTs in the MCE, we consider a 1D LJ chain, moving freely in a 1D box volume $[-L/2,L/2]$. In this case, the pair potential in Hamiltonian (1a) reads

$$U_{\mathrm{pair}}(q)=\frac{1}{2}\sum_{\substack{i,j=1\\ i\neq j}}^{N} U_{\mathrm{LJ}}(|q_i-q_j|),\quad U_{\mathrm{LJ}}(r)=4a\left[\left(\frac{\sigma}{r}\right)^{12}-\left(\frac{\sigma}{r}\right)^{6}\right], \tag{14}$$

where $a,\sigma>0$ are positive parameters. To simplify subsequent formulae, we will measure energy and length in units of the parameters a and $r_0=2^{1/6}\sigma$, where r_0 is the position of the minimum of $U_{\mathrm{LJ}}(r)$. With respect to these units the LJ potential (14) is given by

$$U_{\mathrm{LJ}}(r)=\frac{1}{r^{12}}-\frac{2}{r^6}. \tag{15}$$

For small volumes $L\leqslant 1$ the LJ-force is always repulsive, whereas in the more interesting case of sufficiently large volumes, $L>1$, the LJ-force may also become attracting.

2.3.1. Diatomic LJ molecule

We start by discussing the simplest non-trivial example $N=2$ and $D=1$, where we can calculate the microcanonical TDFs exactly.[5] In this case, the energy E can take values $E_0(L)\leqslant E<\infty$, where the groundstate energy is given by

$$E_0(L)\equiv\min_{(q,p)} H(q,p)=\begin{cases} U_{\mathrm{LJ}}(L), & L\leqslant 1,\\ -1, & L>1. \end{cases} \tag{16}$$

[3]In an ordinary sense, Eq. (13) is defined for even integer values $d>0$ only; however, by employing fractional derivatives [56], its range of validity can be extended to odd integer values $d>0$.

[4]Recently, similar results have been reported for the mean-field spherical spin model by Kastner and Schnetz [57].

[5]The phase volume for the more complicated three-dimensional problem was recently calculated by Umirzakov [58].

A straightforward calculation of the phase volume, based on relative and center-of-mass coordinates, yields

$$\Omega = \frac{2\pi m}{h^2}\left(\frac{L}{11r^{11}} - \frac{1}{10r^{10}} - \frac{2L}{5r^5} + \frac{1}{2r^4} + LrE - \frac{r^2E}{2}\right)\Bigg|_{r_{\min}}^{r_{\max}}, \tag{17a}$$

where the boundary values are given by

$$r_{\min} = X^{-1/6}, \quad r_{\max} = \begin{cases} L, & E \geqslant E_c(L) \equiv U_{\mathrm{LJ}}(L), \\ Y^{-1/6}, & E < E_c(L), \end{cases} \tag{17b}$$

using the convenient abbreviations $X \equiv 1 + \sqrt{1+E}$ and $Y \equiv 1 - \sqrt{1+E}$.

In the case $L \leqslant 1$ we have $r_{\max} = L$ for all energies $E \geqslant E_0$, and, hence, the phase volume $\Omega(E)$ is a smooth function for all permitted energy values. For $L > 1$, however, the boundary value $r_{\max}$ changes its energy dependence at $E = E_c(L)$ in a non-analytic manner, and hence the phase volume $\Omega(E)$ is not analytic at $E = E_c(L)$. The critical curve $E_c(L) \equiv U_{\mathrm{LJ}}(L)$, $L \geqslant 1$ separates a gas-like phase (dissociated state) from the molecular phase (bound state) in the (L, E)-parameter plane. This is illustrated in Fig. 1 and will become particularly evident from the expansions presented in the next two paragraphs. It is worthwhile to stress again that the critical curve $E_c(L)$ arises naturally due to the sudden change in the energy dependence of the phase volume, occurring when the energy E passes the critical curve. The microcanonical caloric curve $T(E)$ is continuous but not differentiable along the critical transition curve $E_c(L)$, which is located in the region of an S-bend or van der Waals-type loop, respectively. Formally, this corresponds to a fourth-order transition.

Super-critical energy values (*dissociated phase*). Using result (17) with $r_2 = L$, corresponding to supercritical energy values $E > E_c(L)$—or region '(1)' in Fig. 1, respectively—we can derive from Eq. (3) the microcanonical EOS, yielding

$$kT = \frac{Z + 24L(X - 5E)/X^{1/6} - 33(X - 2E)/X^{1/3}}{55[L^2 - (E + X)(2LX^{1/6} - 1)/X^{4/3}(1 + E)^{1/2}]}, \tag{18a}$$

$$\frac{pL}{kT} = \frac{110L^2E + 10/L^{10} - 44/L^4 - 2L[X(5X - 22) + 55E]/X^{1/6}}{Z + 11[X(X - 5) + 5E]/X^{1/3} - 2L[X(5X - 22) + 55E]/X^{1/6}}, \tag{18b}$$

where $Z \equiv 55L^2E + 11L^{-4} - L^{-10}$. Taking the high-energy limit at constant volume $V = L$ one finds

$$\lim_{E\to\infty} \frac{kT}{E} = 1, \quad \lim_{E\to\infty} \frac{PL}{kT} = 2, \tag{19}$$

corresponding to the laws for the ideal 1D two-particle gas. Hence, the parameter region $E > E_c(L)$ can be identified as two-particle gas state or dissociated phase, respectively.

Sub-critical energy values (*bound phase*). Because of Eq. (16), the opposite case $E < E_c(L)$—corresponding to region '(3)' in Fig. 1(a)—can only be realized, if $L > 1$ holds; i.e., if the box volume is larger than the distance

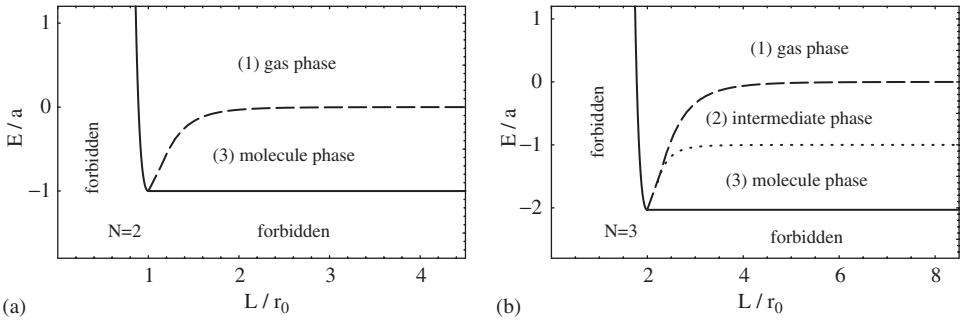

Fig. 1. Microcanonical phase diagrams for the 1D LJ molecules. Energies below the minimum energy $E_0(L)$ (solid line) are forbidden. (a) Diatomic LJ molecule ($N = 2$): the critical curve $E_c(L)$ (dashed line) separates a gas-like (or dissociated) phase from a molecule phase. (b) Triatomic LJ molecule ($N = 3$): the critical curve $E_{c1}(L)$ (dashed line) separates a gas-like (or dissociated) phase from an intermediate (partially bound) phase, enclosed by the critical curves $E_{c1}(L)$ and $E_{c2}(L)$ (dotted line), and a bound molecule phase (3) below $E_{c2}(L)$.

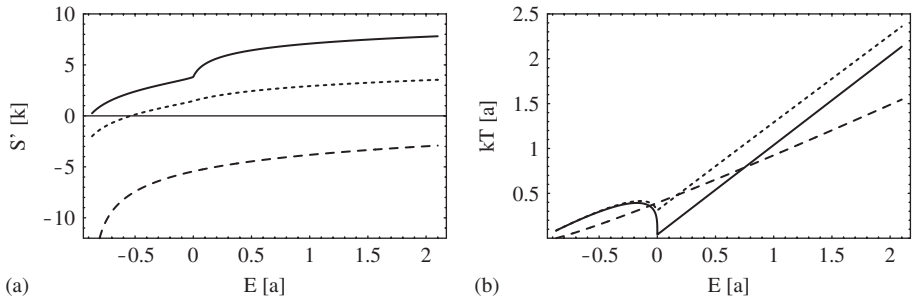

Fig. 2. Microcanonical TDFs for the 1D diatomic LJ molecule ($N = 2$). Energy is measured in units of the binding energy a. Volume $V = L$ is measured in units of the parameter r_0, corresponding to the minimum of the LJ potential. The mass unit is chosen such that $m = 1$. (a) Hertz entropy $S' = S - S_0$ as function of the energy for $L = 20$ (solid line), $L = 3$ (dotted line), and $L = 0.95$ (dashed), where $S_0 = -k \ln[h^2/(mr_0^2 a^2)]$. Note the convex curvature of the solid curve at the transition energy. (b) Caloric curves for $L = 20$ (solid line), $L = 3$ (dotted line), and $L = 0.95$ (dashed). One can readily see the singularity (peak) in the S-bend region, occurring exactly when the critical line $E_c(L) = U_{\mathrm{LJ}}(L)$ in Fig. 1 is crossed.

corresponding to the potential minimum r_0. Again using Eqs. (17), but this time with $r_2 = Y^{-1/6}$, we obtain

$$kT = \frac{3[8Lg(X,Y) - 11f(X,Y)](-E)^{1/3}}{55[X^{1/3} - Y^{1/3} + 2LX^{1/6}(Y^{1/3} - (-E)^{1/6})]}, \tag{20a}$$

$$\frac{pL}{kT} = \frac{8Lg(X,Y)}{8Lg(X,Y) - 11f(X,Y)}, \tag{20b}$$

where we have made use of the abbreviations

$$g \equiv (1+5X)Y^{5/6} - (1+5Y)X^{5/6}, \quad f \equiv (1+2X)Y^{2/3} - (1+2Y)X^{2/3}.$$

Expanding EOS (20b) near the groundstate energy $E_0 = -1$ yields

$$kT = \tfrac{2}{3}(E+1) + \mathcal{O}[(E+1)^2], \tag{21a}$$

$$\frac{P}{kT} = \frac{1}{L-1} + \mathcal{O}[(E+1)^1]. \tag{21b}$$

Eq. (21a) indicates that, at low energy, each momentum variable as well as an approximately harmonic excitation of the relative coordinate carries on average the energy amount $kT/2$. Obviously, this is in agreement with the equipartition theorem for harmonic DOF. Eq. (21b) corresponds to the pressure law for an ideal one-particle gas in the reduced 1D volume $V_{\mathrm{eff}} = L - 1$, reflecting the fact that, at sufficiently low energy values, the two particles form a bound molecule with distance $r \approx 1$ between each other.

In Fig. 2(b) the caloric curves and the pressure law are shown for different fixed values of L and E, respectively. When the volume is large enough, $L \geqslant 1$, the caloric curves exhibit a characteristic convex region (S-bend) and, in particular, also a non-differentiable point (see solid and dotted curves). These kinks occur when the energy passes through the critical value $E_c(L)$.

2.3.2. LJ chains with $N > 2$ particles

Analogous microscopic PTs do also occur in LJ molecules with larger particle numbers. For $N > 2$ it is very difficult or, perhaps, even impossible to express the phase volume (11) in terms of closed functions. Usually, one can perform only one or two of the N integrations analytically, and the remaining integrals have to be calculated numerically, using e.g., Monte–Carlo methods. We employed the Divonne algorithm of the CUBA library [59] to calculate the phase volume for LJ molecules with 3 and 4 particles. We used at least 1 million sample points and partially increased the sample size up to 100 million points for testing. We also cross-checked the results with other deterministic and probabilistic integration algorithms of the CUBA library and found excellent agreement.

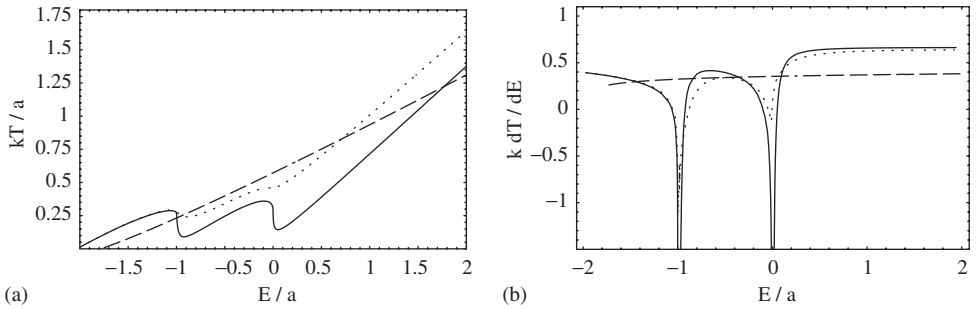

Fig. 3. LJ chain with $N = 3$ particles. (a) The microcanonical caloric curve $T(E)$, and (b) its first derivative for different values of the volume $L = 1.9$ (dashed line), $L = 6$ (dotted line), and $L = 40$ (solid line). $T(E)$ shows two S-bend regions for $L = 6$ and $L = 40$. In these regions, the first derivative $\mathrm{d}T(E)/\mathrm{d}E$ exhibits a lambda peak pointing downward (the second derivative $\mathrm{d}^2T(E)/\mathrm{d}E^2$ has a pole).

Fig. 3 shows the numerically calculated microcanonical caloric curve $T(E)$ of the three-particle LJ chain ($N = 3$) and its first derivative for different values of L. For $L = 1.9$, the caloric curve appears smooth and almost linear. For $L = 6$ and $= 40$, $T(E)$ is still continuous, but shows two S-bend regions around energies $E_{c1} \approx -1$ and $E_{c2} \approx 0$. At these energies, the first derivative of $T(E)$ exhibits a (negative) 'lambda peak', whereas the second derivative diverges.

As in the two-particle case, the phase volume $\Omega(E, L)$ can be written as an integral with an integrand which is analytic for all values of E and L, and integration boundaries which are analytic except for certain values of E and L. A detailed analysis yields the two critical curves

$$E_{c1}(L) = U_{\mathrm{LJ}}\left(\frac{L}{2}\right) + U_{\mathrm{LJ}}\left(\frac{L}{2}\right) + U_{\mathrm{LJ}}(L) \quad \text{if } L \geqslant \left(\frac{2731}{43}\right)^{1/6},$$

$$E_{c2}(L) = U_{\mathrm{LJ}}(r_{c2}(L)) + U_{\mathrm{LJ}}(L - r_{c2}(L)) + U_{\mathrm{LJ}}(L) \quad \text{if } L \geqslant 2\left(\frac{13}{7}\right)^{1/6},$$

where $r_{c2}(L)$ is given by a polynomial equation of degree eighteen, with $r_{c2}(L) \approx -1$ for $L \gg 1$. The resulting phase diagram is shown in Fig. 1(b). One readily identifies three microscopic phases separated by the critical curves $E_{c1}(L)$ and $E_{c2}(L)$.

At high energies $E > E_{c1}(L)$, the system is in a gas-like, fully dissociated phase. The relative positions $r_{21} = |q_2 - q_1|$ and $r_{32} = |q_3 - q_2|$ of the particles are only restricted by the hard-core repulsive part of the interaction potential, but apart from this constraint the particles can move independently inside the remaining volume. In the high-energy limit, one finds $E \approx \frac{3}{2}kT$, corresponding to a quasi-ideal 1D three-particle gas.

For $L > 2(\frac{13}{7})^{1/6}$ and low energies $E_0(L) < E < E_{c2}(L)$, the system is in a bound molecule phase. The relative positions r_{21} and r_{32} are restricted by the interaction potential to be close to the equilibrium position.

For $L > 2(\frac{13}{7})^{1/6}$ and intermediate energy values $E_{c2}(L) < E < E_{c1}(L)$, the system is in a partially dissociated phase. One of the relative positions r_{21} and r_{32} is restricted to be close to its equilibrium value, whereas the other is only restricted by the hard-core repulsive part of the interaction potential and the box volume. Accordingly, one of the three particles may move rather independently inside the box, whereas the other two remain bound to each other.

Although more complicated in detail, the calculations for the four-particle LJ chain are in principle the same as for $N = 3$. We briefly list the main results: For $N = 4$ (and only taking nearest-neighbor interaction into account), three critical lines $E_{c1}(L)$, $E_{c2}(L)$ and $E_{c3}(L)$ divide the (L, E)-plane into four different phases. At high energies or at low volumes $L < L_0$, $L_0 = 3$, the system is in a gas-like phase. At low energies and large volume, the system is in a molecule phase, where the particles can only move as a whole molecule inside the volume. Between the gas phase and the molecule phase, there are now *two* intermediate, or partly dissociated, phases, where the LJ molecule is broken up into two or three parts consisting of one or two particles. For large volumes, the caloric curve $T(E)$ shows three PTs with a continuous first, but discontinuous second derivative. This confirms that the formal order of the microscopic PTs increases with particle number as discussed in Section 2.2.

2.4. Takahashi gas

As another example, let us consider the piecewise linear pair potential

$$u(r) = \begin{cases} +\infty, & |r| = 0, \\ a|r|/r_0, & 0 < |r| \leqslant r_0, \\ 1, & |r| > r_0, \end{cases} \tag{22}$$

where a and r_0 are positive parameters. In the literature this model is known as the Takahashi gas [44]. The potential u from Eq. (22) is qualitatively similar to the LJ potential, but, unlike U_{LJ}, it allows to calculate the exact TDFs for both MCE and CE in the case $N = 2$. The Takahashi gas is, therefore, particularly well suited for studying the differences between the two ensembles.

To keep subsequent calculations as simple as possible, we will measure energy and length in units of a and r_0 from now on (r_0 now defines the range of the potential). With respect to these units, the potential in Eq. (22) simplifies to

$$u(r) = \begin{cases} +\infty, & |r| = 0, \\ |r|, & 0 < |r| \leqslant 1, \\ 1, & |r| > 1, \end{cases} \tag{23}$$

and, in contrast to Eq. (16), the groundstate energy is now given by $E_0(L) = 0$. A straightforward calculation of the phase volume yields

$$\Omega = \frac{\pi m}{3h^2} \begin{cases} L^2(3E - L), & E > E_c(L), \quad L \leqslant 1, \\ 3L[L(E-1)+1] - 1, & E > E_c(L), \quad L > 1, \\ E^2(3L - E), & E \leqslant E_c(L), \end{cases} \tag{24}$$

where the critical energy curve is given by $E_c(L) \equiv u(L)$. Note that, compared with the LJ potential from Section 2.3.1, we must now additionally distinguish the cases $L \leqslant 1$ and $L > 1$, but this is only because the piecewise linear potential is not differentiable at $r = 1$. However, analogous to the case of the LJ potential, the critical curve $E_c(L) = u(L)$ separates a gas-like phase (dissociated state) from the molecule phase (bound state) in the (L, E)-parameter plane. This becomes evident from the microcanonical EOS:

$$\frac{1}{kT} = \begin{cases} \dfrac{3}{3E - L}, & E > E_c(L), \quad L \leqslant 1, \\ \dfrac{3L^2}{3L[L(E-1)+1] - 1}, & E > E_c(L), \quad L > 1, \\ \dfrac{2}{E} + \dfrac{1}{E - 3L}, & E \leqslant E_c(L), \end{cases} \tag{25a}$$

$$\frac{P}{kT} = \begin{cases} \dfrac{3L - 6E}{L^2 - 3LE}, & E > E_c(L), \quad L \leqslant 1, \\ \dfrac{6L(E-1) + 3}{3L[L(E-1)+1] - 1}, & E > E_c(L), \quad L > 1, \\ \dfrac{3}{3L - E}, & E \leqslant E_c(L). \end{cases} \tag{25b}$$

Taking the high-energy limits of Eqs. (25) at constant volume $V = L$ one finds

$$\lim_{E\to\infty} \frac{E}{kT} = 1, \quad \lim_{E\to\infty} \frac{PL}{kT} = 2, \tag{26}$$

corresponding to the laws for the ideal 1D two-particle gas. Hence, the parameter region $E > E_c(L)$ can be referred to as gas-like or dissociated phase, respectively.

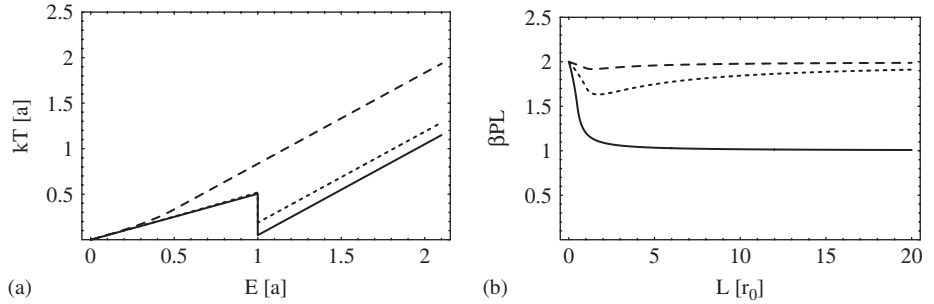

Fig. 4. Microcanonical TDFs for the 1D diatomic ($N = 2$) Takahashi gas. (a) Caloric curves for $L = 20$ (solid line), $L = 5$ (dotted), and $L = 0.5$ (dashed). One can see the jump singularity for $L > 1$, occurring exactly when the critical line $E_c(L) = u(L)$ is crossed. (b) Isoenergetic pressure curves for $E = 0.5$ (solid line), $E = 1.5$ (dotted), and $E = 5.0$ (dashed), where $\beta \equiv (kT)^{-1}$. The local minimum is observable only if $E/a \gtrsim 1$. In the limit $L \to \infty$ the particles behave as an ideal two-particle (one-particle) gas, if they are in the dissociated phase $E > a$ (bound phase $E < a$).

In the opposite case, $E \leqslant E_c(L)$, a low-energy expansion of the EOS near the groundstate energy $E_0 = -1$ yields

$$\frac{P}{kT} = \frac{1}{L} + \mathcal{O}(E^1). \tag{27}$$

Neglecting terms of higher order, Eq. (27) corresponds to the pressure law for an ideal one-particle gas. This reflects that at sufficiently low energy the two particles form a bound LJ-type molecule. Compared with the results of the preceding section, a slight difference is given by the fact that in the LJ case the particles have a non-vanishing distance in the groundstate, see Eq. (21b).

In Fig. 4(a) and (b) the caloric curves and the pressure law are shown for different fixed values of L and E, respectively. In particular, in Fig. 4(a) one can see that the caloric curves exhibit a singularity, when the energy passes through the critical value $E_c(L)$. More exactly, for $L \leqslant 1$ the caloric curves are continuous but not differentiable at $E = E_c(L)$, corresponding to a third-order PT. By contrast, in the complementary case $L > 1$, the caloric curves become discontinuous at $E_c(L)$, corresponding to a second-order PT (which is a consequence of the additional singularity at $r = 1$ and the vanishing gradient of the piecewise linear potential at $r > 1$).

In the next section, we are going to study the relationship between this singular microcanonical PT and the critical behavior of the corresponding systems in the CE.

3. Smooth PTs in the CE

Although referring to different physical conditions, MCE and CE may yield (almost) identical TDFs for well-behaved systems with a large number of DOF $d \to \infty$. However, this 'equivalence' between the different statistical ensembles does usually not hold for systems with a small number of DOF [25,43,45,60,61]. Hence, one has to describe the thermodynamics of small systems by the statistical ensemble which actually corresponds to the given physical conditions.

3.1. The canonical ensemble

Considering the CE is appropriate if the system under investigation is coupled to an infinite heat bath [45,62–64]. The surrounding heat bath (thermostat) keeps the temperature of the particles constant, but causes energy fluctuations $\delta E > 0$ around the energy mean value $\bar{E}$. Consequently, singularities in the TDFs may only exist in the thermodynamic limit with $N, E \to \infty$, such that $e = E/N$ and $n = N/V$ remain constant and $\delta e \to 0$; i.e., for a finite system with $N < \infty$ the heat bath smoothens the singularities due to non-vanishing fluctuations δe. Nevertheless, it is possible to define and to classify 'smooth' PTs by virtue of the DOZ scheme [34], discussed below.

Given a Hamiltonian of the form (1a), the canonical partition function is defined by

$$\mathscr{Z}_{\mathrm{C}}(\beta, V) = \frac{1}{N!h^d}\int_{\mathbb{R}^d} \mathrm{d}q \int_{\mathbb{R}^d} \mathrm{d}p \exp[-\beta H(q,p;V)], \tag{28}$$

where $\beta \equiv (kT)^{-1}$. The external control variables are now (T, V) or (β, V), respectively. When $\mathscr{Z}_{\mathrm{C}}(\beta, V)$ is known, (mean) energy and pressure of the CE are obtained by differentiation

$$\bar{E} \equiv -\frac{\partial}{\partial\beta}\ln \mathscr{Z}_{\mathrm{C}}, \quad \bar{P} \equiv -\frac{\partial F}{\partial V}, \tag{29}$$

where $F \equiv -kT \ln \mathscr{Z}_{\mathrm{C}}$ is the free energy. For convenience, we are going to drop the over-bars and simply write E and P in the next section (over-bars will be reinstated occasionally, e.g., when comparing microcanonical and canonical quantities).

3.2. Classification of canonical PTs in the DOZ scheme

According to Yang and Lee [8,9], DOZ of the grandcanonical partition function determines the PTs in the grandcanonical ensemble. Later on, a similar approach has been employed by Fisher [10] and Grossmann and Rosenbauer [11] to identify and classify PTs in the CE. They considered the distribution of complex zeros $\tilde{\beta}_k$ of the canonical partition function $\mathscr{Z}_{\mathrm{C}}(\tilde{\beta})$, taken as complex function of the complex inverse temperature

$$\tilde{\beta} = \beta + i\tau \quad (\beta > 0).$$

For finite systems, one can show that there are no zeros on the positive real axis, i.e., $\Im(\tilde{\beta}_k) \neq 0 \ \forall k$. In the thermodynamic limit, however, certain points β_c on the real β-axis may become limiting values of the DOZ. By studying how the zeros condense near the β-axis, one can characterize the PT.

Although for small systems there are, strictly speaking, no non-analytic PTs in the CE, it may nevertheless be helpful to distinguish different thermodynamic phases [31,32]. The DOZ classification scheme of Bohrmann et al. [34] is based on the idea that the complex zeros $\tilde{\beta}_k$ closest to the real β-axis can be employed to estimate the DOZ behavior in the thermodynamic limit. The extrapolated limiting values β_c are used to define the 'smooth' canonical PT of the finite system. To be more specific, one first numbers the complex zeros $\tilde{\beta}_k$, $k = 1, 2, \ldots$ of the canonical partition function $\mathscr{Z}_{\mathrm{C}}(\tilde{\beta})$ according to their distance to the real β-axis, and then calculates the quantities

$$\gamma = \frac{\beta_2 - \beta_1}{\tau_2 - \tau_1}, \tag{30a}$$

$$\phi_k = \frac{1}{2}\left(\frac{1}{|\tilde{\beta}_k - \tilde{\beta}_{k-1}|} + \frac{1}{|\tilde{\beta}_{k+1} - \tilde{\beta}_k|}\right), \quad k = 2, 3, \ldots, \tag{30b}$$

$$\alpha = \frac{\log(\phi_3) - \log(\phi_2)}{\log(\tau_3) - \log(\tau_2)}, \tag{30c}$$

$$\beta_c = \beta_1 - \gamma\tau_1. \tag{30d}$$

These quantities characterize the DOZ near the real β-axis. According to the scheme of Borrmann et al. [34], a first-order transition at temperature $T_c = (k\beta_c)^{-1}$ appears if $\alpha = 0$ and $\gamma = 0$, whereas values $1 > \alpha > 0$ correspond to second-order transitions, and $\alpha > 1$ to even higher-order transitions in the original Ehrenfest classification. In order to actually observe a singular PT in the Ehrenfest sense, it is required that $\tau_1 \to 0$ in the thermodynamic limit.

A similar classification scheme for smooth canonical PTs in small systems, based on the average cumulative density of zeros of the canonical partition function, has been proposed by Janke, Kenna et al. [38,65]. Alves et al. [36] compared both approaches for a variety of model systems. In the following, however, we will refer to the DOZ-scheme by Borrmann et al. [34] in order to classify PTs in the CE of a small system. In particular, we aim to compare the DOZ-classification with the MCE results obtained for the Takahashi gas.

3.3. Takahashi gas

We first calculate the canonical TDFs for the Takahashi model from Section 2.4, corresponding to two point-like particles, $N = 2$, confined in a 1D volume $V = L$ and interacting via the (rescaled) piecewise linear pair potential from Eq. (23). For $L \leqslant 1$, we find explicitly

$$\mathcal{Z}_C = 2\frac{m\pi}{h^2\beta^3}(e^{-\beta L} + \beta L - 1), \tag{31a}$$

and in the opposite case, that is for $L > 1$,

$$\mathcal{Z}_C = 2\frac{m\pi}{h^2\beta}\left\{\frac{1}{\beta^2}[e^{-\beta}(1+\beta-\beta L) + \beta L - 1] + \frac{e^{-\beta}}{2}(L-1)^2\right\}. \tag{31b}$$

Accordingly, one obtains the following canonical EOS:

$$E = \begin{cases} \dfrac{3 + \beta L + e^{\beta L}(2\beta L - 3)}{\beta[1 + e^{\beta L}(\beta L - 1)]}, & L \leqslant 1, \\ \dfrac{6\beta + (6 - 4\beta L)(1 - e^{\beta}) + \beta^2(L-1)[L - 3 + \beta(L-1)]}{\beta\{1 + [1 - \beta(L-1)]^2 + 2e^{\beta}(\beta L - 1)\}}, & L > 1, \end{cases} \tag{32a}$$

$$P = \begin{cases} \dfrac{e^{\beta L - 1}}{e^{\beta L}(\beta L - 1) + 1}, & L \leqslant 1, \\ \dfrac{2[e^{\beta} - 1 + \beta(L-1)]}{1 + [1 - \beta(L-1)]^2 + 2e^{\beta}(\beta L - 1)} & L > 1. \end{cases} \tag{32b}$$

In the high-temperature limit, corresponding to $\beta \to 0$ at constant volume $V = L$, one finds

$$\lim_{\beta\to 0} \beta E = 1, \quad \lim_{\beta\to 0} \beta P L = 2, \tag{33}$$

i.e., the system behaves like an ideal 1D two-particle gas in this limit.

Fig. 5 shows several curves, corresponding to the thermodynamic laws (32). One may notice a strong local increase in the solid caloric curve of Fig. 5(a). This behavior is associated with a smooth canonical PT in the DOZ scheme of Borrmann et al. [34]. To see this, we next determine the complex zeros of the complex partition function $\mathcal{Z}_C(\beta + i\tau, L)$ for $L > 1$ from Eq. (31). Fig. 6(a) shows the corresponding numerical results found with Mathematica [66] for $L = 20$, by using a contour plot of the function $|\mathcal{Z}_C(\beta + i\tau, L)|$. Since the zeros of the partition function are complex conjugate [34], only the zeros in the upper complex half-plane are shown.

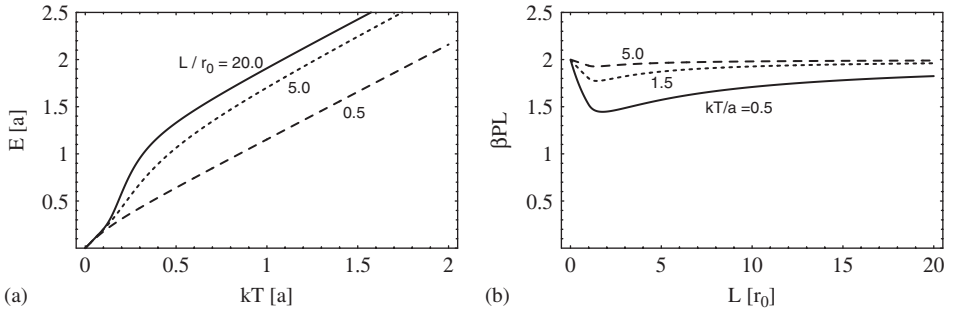

Fig. 5. Canonical TDFs for the 1D diatomic Takahashi gas. Mean energy E and thermal energy kT are given in units of the binding energy a. The volume $V = L$ is measured in units of the parameter r_0, corresponding to the range of the potential, and the mass unit is chosen such that $m = 1$ holds. (a) Caloric curves for different fixed values of L. (b) Pressure law for different fixed temperature values kT. Note, that $\beta PL \to 2$ for $L \to \infty$, corresponding to the law of the ideal two-particle gas.

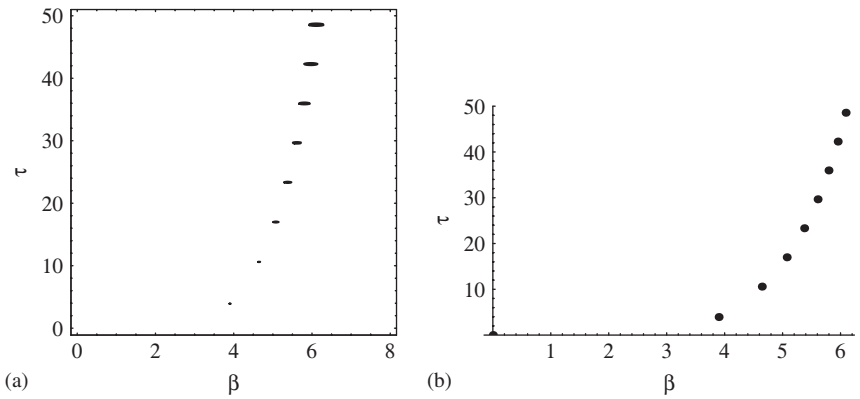

Fig. 6. Complex zeros of canonical distribution function $\mathscr{Z}_C(\beta+i\tau)$ for the 1D diatomic molecule with the piecewise linear pair interaction potential $u(r)$ from Eq. (22). Quantities β and τ are given in units of the inverse binding energy a^{-1}. (a) Numerically determined zeros in the upper half-plane obtained with Mathematica for $L/r_0 = 20$. (b) Analytic results based on the asymptotic series expansion of $\mathscr{Z}_C$ at $L/r_0 \to \infty$, see Eq. (35). As evident from these two diagrams, the analytic estimate agrees well with the numerically determined results.

Table 1
Canonical PT parameters according to the DOZ scheme [34] for the 1D diatomic molecule with piecewise linear interaction potential from Eq. (22)

$L\ [r_0]$	α	γ	$\beta_c\ [a^{-1}]$	$kT_c\ [a]$	$E(T_c)\ [a]$
2×10^{1}	0.054	0.112	3.5	0.290	0.922
2×10^{3}	0.052	0.052	9.0	0.111	0.688
2×10^{5}	0.034	0.028	14.1	0.071	0.620
2×10^{10}	1.1×10^{-2}	9.1×10^{-3}	26.3	0.0381	0.56210
2×10^{100}	2.4×10^{-5}	1.1×10^{-4}	235.7	0.0042	0.50643
2×10^{1000}	2.5×10^{-8}	1.2×10^{-6}	2310.3	0.0004	0.50065

For $L\to\infty$ the numerical results suggest that $\alpha\to0$, $\gamma\to0$ and $kT_c/a\to0$.

To also obtain an analytic estimate for the DOZ in the more interesting case $L\gg1$, we expand the partition function (31b) near $L\to\infty$, and find

$$\mathscr{Z}_C(\tilde{\beta},L)=\frac{m\pi L^2}{h^2\tilde{\beta}}\left\{e^{-\tilde{\beta}}\left[1+\frac{2}{\tilde{\beta}L}(e^{\tilde{\beta}}-\tilde{\beta}-1)\right]+\mathscr{O}(L^{-2})\right\}. \tag{34}$$

Thus, neglecting terms of $\mathscr{O}(L^{-2})$, the zeros of $\mathscr{Z}_C(\tilde{\beta},L)$ are given by

$$\tilde{\beta}_k=\frac{2}{L-2}-\mathrm{ProdLog}\left[-k,\frac{2}{L-2}\exp\left(\frac{2}{L-2}\right)\right],\quad k=\pm1,\pm2,\ldots, \tag{35}$$

where $\mathrm{ProdLog}[k,z]$ is the kth solution for w in $z=w\exp(w)$. The result (35) is valid for $L\gg1$, and in Fig. 6(b) we plotted $\tilde{\beta}_k$ for $1\leqslant k\leqslant8$. By comparing Fig. 6(a) and (b) it becomes evident that for $L\geqslant20$ the analytic estimate from Eq. (35) is in good agreement with the numerical results.

Using Eq. (35) we can calculate the characteristic quantities α,β_c,γ from Eqs. (30), required for the DOZ classification. Table 1 shows a summary of the results for different values of the volume parameter L. The critical temperature is given by $kT_c=1/\beta_c$ and E_c is obtained by inserting β_c into the energy equation (32a). According to the DOZ scheme, for $1\ll L<\infty$ we find $0<\alpha<1$, corresponding to a canonical second-order PT. However, for $L\to\infty$ we observe that $\alpha\to0$, $\gamma\to0$ indicating that in this limit the transition converges to first order. Moreover, as evident from the last two columns in Table 1, for increasing volume L the critical temperature vanishes, $T_c\to0$, while the corresponding energy values $E(T_c)$ approach the value 0.5. However,

by *first* taking the limit $L \to \infty$ in Eq. (32a), we find that the corresponding asymptotic caloric curve is given by

$$\lim_{L\to\infty} E = 1 + \beta^{-1} = 1 + kT, \quad T > 0. \tag{36}$$

Inserting T_c into the rhs of this equation and letting $T_c \to 0$, we obtain $\bar{E}_c = 1$, which is in agreement with microcanonical result $E_c(L = \infty) = 1$, and corresponds to the dissociation energy. In particular, the latter result means that, in the case of a very large volume, very small energy fluctuations (requiring $T > 0$) suffice to permanently break up the molecule. On the other hand, the system becomes deterministic at $T = 0$, and, correspondingly, the mean energy of the CE is then always given by the groundstate value $E_0 = 0$, representing the bound state [formally this corresponds first taking the limit $T \to 0$ in Eq. (32a)]. The apparent convergence to 0.5 in the last column of Table 1 just reflects the fact that for Eq. (32a) the two limits $T \to 0$ and $L \to \infty$ do not commute.

4. Summary and discussion

In this paper we have studied PTs-like phenomena in small systems, characterized by a finite number of DOF. The main objective was to clarify similarities and differences that arise when considering either the MCE, corresponding to a thermally isolated system, or the CE, corresponding to a system in contact with an infinite heat bath.

4.1. Microscopic PTs in the MCE

In Section 2 it was shown that the *microcanonical* thermodynamic functions (TDFs) of a small system can exhibit complex oscillatory behavior and singularities (non-analyticities). Analogous to *macroscopic* phase transitions (PTs), such non-analytic points can be interpreted as *microscopic* PTs in the MCE.[6] To illustrate the physical meaning of such microscopic PTs, we calculated the microcanonical TDFs for two slightly different 1D toy models (LJ and Takahashi gas). For both systems one can identify critical energy curves $E_c(L)$ along which the primary microcanonical thermodynamic potential—the Hertz entropy—is non-analytic, reflected by kinks or discontinuities in the TDFs. In these models the microscopic PTs separate energetically different dissociation states. Their number and formal order increases with increasing particle number N [57]. In general, our results indicate that, *typically*, *microscopic PTs in the MCE are accompanied by strong qualitative changes of the thermodynamic observables*, *as e.g.*, *rapid drop-offs or oscillations of temperature and heat capacities*, see Fig. 3(a). These effects should be observable in suitably designed evaporation experiments, realizing the conditions of the MCE (similar to those of Schmidt et al. [30], but without heat bath).

For the model systems considered in this paper, a non-analyticity in the TDFs is characterized by a critical energy curve $E_c(L)$. Mathematically, such critical curves $E_c(L)$ arise due to the integration over the Θ-function in the definition of the microcanonical phase volume Ω. The Θ-function in Eq. (11) effectively constrains the range of the integration to the subset

$$\mathscr{A} = \{(q_1, \ldots, q_d) \in \mathbb{R}^d \mid E - U(q_1, \ldots, q_d; V) \geqslant 0\} \tag{37}$$

in the configuration space; i.e., $\mathscr{A}$ is the energetically permitted configuration space region. Hence, a singularity in the microcanonical TDFs may arise whenever $\mathscr{A}$ changes its geometry or 'shape' in an irregular manner during a small variation of the control parameters E and V. One possible origin for this may be a change in the topology of $\mathscr{A}$ (as discussed by Pettini et al. [18–20]). For the models considered here, however, the topology of $\mathscr{A}$ remains unaffected and another general mechanism is at work. To illustrate this in more detail, we recall the example from Section 2.3.1, corresponding to the two-particle LJ gas. In this case, the set

[6]Formally, such singularities can be softened by using an 'artificially' smoothened box potential. However, this would *not* affect experimentally observable effects, as, e.g., a drop-off of the temperature (mean kinetic energy) when the energy level for the next dissociation step is crossed. Loosely speaking, employing a smoothened box potential in the thermodynamic analysis of a small system is similar to avoiding the thermodynamic limit when being interested in PTs of large systems.

$\mathscr{A}$ can be expressed as

$$\mathscr{A} = \{(q_1, q_2) \in \mathbb{R}^2 \mid (q_1, q_2) \in [-L/2, L/2]^2 \wedge E - U_{\mathrm{LJ}}(q_1 - q_2) \geqslant 0\},$$

where U_{LJ} is given by Eq. (14). The first constraint for (q_1, q_2) reflects the box potential, whereas the second constraint arises from the interaction potential. For $E < E_c(L)$, $\mathscr{A}$ consists of the two diagonal 'strips'

$$\mathscr{A}_{\pm} = \{(q_1, q_2) \in [-L/2, L/2]^2 \wedge r_-(E) \leqslant \pm(q_1 - q_2) \leqslant r_+(E)\}, \tag{38}$$

where $r_-(E) > 0$ and $r_+(E) > 0$ denote the classical turning points of the LJ potential. The 'strips' $\mathscr{A}_{\pm}$ are bounded by the box potential on two sides, whereas the other two boundaries are determined by the LJ interaction potential. For $E > E_c(L)$, however, the regions $\mathscr{A}_{\pm}$ become triangles, bounded by the box potential on two sides and by the interaction potential on the remaining side:

$$\mathscr{A}_{\pm} = \{(q_1, q_2) \in [-L/2, L/2]^2 \wedge r_-(E) \leqslant \pm(q_1 - q_2)\}.$$

Evidently, $\mathscr{A}$ changes its geometry dramatically, when the energy passes through the critical energy $E_c(L)$, thereby giving rise to the microscopic PT. For a sufficiently large volume $L \gg r_0$, where r_0 is the range of the pair interaction, this non-analytic transformation of $\mathscr{A}$ at the dissociation energy is accompanied by a change of $\mathscr{A}$'s effective dimensionality. Here, we mean by 'effective dimensionality' the number of orthogonal configuration space directions in which the set $\mathscr{A}$ extends comparably to the system size L. For energy values $E \ll E_c(L)$, the 'strips' $\mathscr{A}_{\pm}$ defined by Eq. (38) are very narrow compared to the system size L, and, hence, $\mathscr{A} = \mathscr{A}_+ \cup \mathscr{A}_-$ is effectively 1D. When the energy approaches $E_c(L)$ from below, the (average) width of the two subsets $\mathscr{A}_{\pm}$ grow very rapidly, and for $E = E_c(L)$, they become triangles whose size is of the order of L^2; i.e., the set $\mathscr{A}$ is effectively two-dimensional for $E \geqslant E_c(L)$. In particular, it is this very rapid growth of $\mathscr{A}$—or Ω, respectively—which leads to a negative slope of the caloric curve $T(E, V)$ in the vicinity of the dissociation energy $E_c(L)$.[7]

4.2. Comparison with the CE

In contrast to the microcanonical TDFs, singular PTs cannot occur in the CE of a finite system [8,9,11–13,41,42]. This is a consequence of the two completely different physical conditions, underlying MCE and CE, respectively [45,25]. In spite of lacking sharp transitions, it is useful to distinguish different thermodynamic 'phases', when considering CEs of finite systems [31,32]. Following the proposal of Borrmann et al. [34], we determined the DOZ for the canonical partition function of the two-particle Takahashi gas (Section 3) and found a 'smooth' canonical second-order PT (according to the DOZ classification scheme), provided the volume L is large compared to the range of the potential, but still finite; for $L \to \infty$ the canonical PT changes to first order in the DOZ scheme.

In principle, however, there exist important differences between the smooth PTs in the CE and the singular microscopic PTs in the MCE: Smooth canonical PTs can be viewed as direct finite size counterparts of macroscopic PTs. In particular, for N particle systems as discussed in this paper the DOZ-scheme usually yields only one transition point. Furthermore, the DOZ-order of the transition point is typically close to one or two. By contrast, when considering the corresponding isolated system (i.e., the MCE), both the number and the formal order of the singular microscopic PTs increase approximately proportional to the particle number (since microscopic PTs signal each dissociation step separately). Such differences notwithstanding, canonical and microcanonical partition functions are linked by a Laplace transformation, which suggests that (not only for small systems) there might exist a direct connection between the canonical DOZ and the appearance of microscopic non-analyticities in microcanonical entropy (see also [67] for a discussion of this hypothesis).

To conclude with, if one wishes to describe small systems by means of a thermodynamic approach, then the non-equivalence of the different statistical ensembles [43] renders necessary to specify in advance, whether or not a heat bath (thermostat) is coupled to the small system under consideration. The discussion in the present paper has focussed on two extreme limit cases, corresponding to a vanishing heat bath (MCE) and an infinite

[7]This also explains why microscopic PTs appear more pronounced for larger L.

heat bath (CE). In the future, it would also be interesting to study PT-like phenomena in small systems coupled to a finite heat bath [68–70], e.g., on the basis of Tsallis' generalized statistics [71–73].

Acknowledgments

The authors thank W. Ebeling, D.H.E. Gross, P. Hänggi, P. Talkner and an anonymous referee for numerous helpful remarks and suggestions.

References

[1] L.P. Kadanoff, W. Götze, D. Hamblen, R. Hecht, E.A.S. Lewis, V.V. Palciauskas, M. Rayl, J. Swift, D. Aspnes, J. Kane, Static phenomena near critical points: theory and experiment, Rev. Mod. Phys. 39 (2) (1967) 395.
[2] J.L. Lebowitz, Statistical mechanics, two central issues, Rev. Mod. Phys. 71 (2) (1999) S351.
[3] P. Ehrenfest, T. Ehrenfest, The conceptual foundation of the statistical approach in mechanics, Cornell University Press, Ithaca, NY, 1959 (reprint of german 1912 edition).
[4] J.E. Mayer, The statistical mechanics of condensing systems. I, J. Chem. Phys. 5 (1937) 67.
[5] J.E. Mayer, P.G. Ackermann, The statistical mechanics of condensing systems. II, J. Chem. Phys. 5 (1937) 74.
[6] J.E. Mayer, S.F. Harrison, The statistical mechanics of condensing systems. III, J. Chem. Phys. 5 (1937) 87.
[7] S.F. Streeter, J.E. Mayer, The statistical mechanics of condensing systems. VI, J. Chem. Phys. 7 (1939) 1025.
[8] C.N. Yang, T.D. Lee, Statistical theory of equations of state and phase transitions. I. Theory of condensation, Phys. Rev. 87 (3) (1952) 404.
[9] T.D. Lee, C.N. Yang, Statistical theory of equations of state and phase transitions. II. Lattice gas and Ising model, Phys. Rev. 87 (3) (1952) 410.
[10] M.E. Fisher, Theory of critical point singularities, in: M.S. Green (Ed.), Critical Phenomena: Proceedings of the 51st Enrico Fermi Summer School, Varenna, Italy, Academic Press, New York, 1971, p. 1.
[11] S. Grossmann, W. Rosenhauer, Temperature dependence near phase transitions in classical and quantum mechanical canonical statistics, Z. Phys. 207 (1967) 138.
[12] S. Grossmann, W. Rosenhauer, Phase transitions and the distribution of temperature zeros of the partition function, Z. Phys. 218 (1969) 437.
[13] S. Grossmann, V. Lehmann, Phase transitions and the distribution of temperature zeros of the partition function, Z. Phys. 218 (1969) 449.
[14] L. Casetti, E.G.D. Cohen, M. Pettini, Exact results on topology and phase transitions, Phys. Rev. E 65 (2002) 036112.
[15] A.C.R. Teixeira, D.A. Stariolo, Topological hypothesis: the simplest case, Phys. Rev. E 70 (2004) 016113.
[16] M. Kastner, Unattainability of a purely topological criterion for the existence of a phase transition for nonconfining potentials, Phys. Rev. Lett. 93 (2004) 150601.
[17] R. Franzosi, M. Pettini, Theorem on the origin of phase transitions, Phys. Rev. Lett. 92 (2004) 060601.
[18] R. Franzosi, M. Pettini, L. Spinelli, Topology and phase transitions I. Theorem on a necessary relation, math-ph/0505057, 2005.
[19] R. Franzosi, M. Pettini, Topology and phase transitions II. Entropy and topology, math-ph/0505058, 2005.
[20] L. Angelani, L. Casetti, M. Pettini, G. Ruocco, F. Zamponi, Topology and phase transitions: from an exactly solvable model to a relation between topology and thermodynamics, Phys. Rev. E 71 (2005) 036152.
[21] T.L. Hill, Thermodynamics of Small Systems, vol. I/ II, Dover, New York, 1994, reprint.
[22] J.L. Lebowitz, J.K. Percus, Thermodynamic properties of small systems, Phys. Rev. 124 (6) (1961) 1673.
[23] D.J. Wales, R.S. Berry, Coexistence in finite systems, Phys. Rev. Lett. 73 (21) (1994) 2875.
[24] D.J. Wales, J.P.K. Doye, Coexistence and phase separation in clusters: from the small to the not-so-small regime, J. Chem. Phys. 103 (1995) 3061.
[25] D.H.E. Gross, Micro-canonical thermodynamics, World Scientific Lecture Notes in Physics, vol. 66, World Scientific, Singapore, 2001.
[26] M. Klindworth, A. Melzer, A. Piel, V.A. Schweigert, Laser-excited intershell rotation of finite coloumb clusters in a dusty plasma, Phys. Rev. B 61 (12) (2000) 8404.
[27] A. Melzer, M. Klindworth, A. Piel, Normal modes of 2d finite clusters in complex plasmas, Phys. Rev. Lett. 87 (2001) 115002.
[28] M.H. Anderson, J.R. Ensher, M.R. Matthews, C.E. Wiedman, E.A. Cornell, Observation of Bose–Einstein condensation in a dilute atomic vapor, Science 269 (1995) 198.
[29] K.B. Davis, M.-O. Mewes, M.R. Andrews, N.J. van Druten, D.S. Durfee, D.M. Kurn, W. Ketterle, Bose–Einstein condensation in a gas of sodium atoms, Phys. Rev. Lett. 75 (1995) 3969.
[30] M. Schmidt, T. Hippler, J. Donges, W. Kronmüller, B. von Issendorff, H. Haberland, P. Labastie, Caloric curve across the liquid-to-gas change for sodium clusters, Phys. Rev. Lett. 87 (2001) 203402.
[31] V.M. Bedanov, F.M. Peeters, Ordering and phase transitions of charged particles in a classical finite two-dimensional system, Phys. Rev. B 49 (4) (1994) 2667.

[32] O.S. Vaulina, S.V. Vladimirov, O.F. Petrov, V.E. Fortov, Criteria of phase transitions in a complex plasma, Phys. Rev. Lett. 88 (24) (2002) 245002.
[33] F. Dalfovo, S. Giorgini, L.P. Pitaevskii, S. Stringari, Theory of Bose–Einstein condensation in trapped gases, Rev. Mod. Phys. 71 (3) (1999) 463.
[34] P. Borrmann, O. Mülken, J. Harting, Classification of phase transitions in small systems, Phys. Rev. Lett. 84 (16) (2000) 3511.
[35] O. Mülken, H. Stamerjohanns, P. Borrmann, Origins of phase transitions in small systems, Phys. Rev. E 64 (2001) 047105.
[36] N.A. Alves, J.P.N. Ferrite, U.H.E. Hansmann, Numerical comparison of two approaches for the study of phase transitions in small systems, Phys. Rev. E 65 (2002) 036110.
[37] D.H.E. Gross, Micro-canonical thermodynamics and statistical fragmentation of dissipative systems—the topological structure of the n-body phase space, Phys. Rep. 279 (1997) 119.
[38] W. Janke, R. Kenna, The strength of first and second order phase transitions from partition function zeroes, J. Stat. Phys. 102 (2001) 1211.
[39] D. Ruelle, Statistical Mechanics, World Scientific, Singapore, 1999.
[40] M. Pleimling, H. Behringer, Microcanonical analysis of small systems, Phase Transitions 78 (2005) 787.
[41] L. van Hove, Sur l'integrale de configuration pour les systemes de particules a une dimension, Physica (Amsterdam) 16 (1950) 137.
[42] J.A. Cuesta, A. Sánchez, General non-existence theorem for phase transitions in one-dimensional systems with short range interactions, and physical examples of such transitions, J. Stat. Phys. 115 (3/4) (2004) 869.
[43] M. Costeniuc, R.S. Ellis, H. Touchette, B. Turkington, The generalized canonical ensemble and its universal equivalence with the microcanonical ensemble, J. Stat. Phys. 119 (5/6) (2005) 1283.
[44] C.J. Thomson, Phase transitions and critical phenomena, One-dimensional models—Short Range Forces, vol. 1, Academic Press, 1972, p. 177 (chapter 5).
[45] R. Becker, Theory of Heat, Springer, New York, 1967.
[46] K. Huang, Statistical Mechanics, Wiley, New York, 1963.
[47] A. Münster, Statistical Thermodynamics, vol. 1, Springer, Berlin, Heidelberg, New York, 1969.
[48] E.M. Pearson, T. Halicioglu, W.A. Tiller, Laplace-transform technique for deriving thermodynamic equations from the classical microcanonical ensemble, Phys. Rev. A 32 (5) (1985) 3030.
[49] T. Cagin, J.R. Ray, Fundamental treatment of molecular-dynamics ensembles, Phys. Rev. A 37 (1988) 247.
[50] P. Hertz, Über die mechanischen Grundlagen der Thermodynamik, Ann. Phys. (Leipzig) 33 (1910) 225.
[51] P. Hertz, Über die mechanischen Grundlagen der Thermodynamik, Ann. Phys. (Leipzig) 33 (1910) 537.
[52] V.L. Berdichevsky, Thermodynamics of Chaos and Order, vol. 90, Addison Wesley Longman, Essex, England, 1997.
[53] V.L. Berdichevsky, M.v. Alberti, Statistical mechanics of Hénon-Heiles oscillators, Phys. Rev. A 44 (2) (1991) 858.
[54] A.B. Adib, Adiabatic invariance with first integrals of motion, Phys. Rev. E 66 (2002) 047101.
[55] P. Ehrenfest, Phase changes classified according to singularities of the thermodynamic potential, Proc. Amsterdam Acad. 36 (1933) 153.
[56] J.L. Lavoie, T.J. Osler, R. Trembley, Fractional derivatives and special functions, SIAM Rev. 18 (2) (1976) 240.
[57] M. Kastner, O. Schnetz, On the mean-field spherical model, J. Stat. Phys. 122(6) (2006) 1195.
[58] I.H. Umirzakov, Exact equilibrium statistical mechanics of two particles interacting via Lennard-Jones and Morse potentials, Phys. Rev. E 61 (2000) 7188.
[59] T. Hahn, Cuba—a library for multidimensional numerical integration, hep-ph/0404043, 2004.
[60] W. Nolting, Statistische Physik, Grundkurs Theoretische Physik, vol. 6, Vieweg, Braunschweig, Wiesbaden, 1998.
[61] L.D. Landau, E.M. Lifshitz, Statistical Physics, third ed., Course of Theoretical Physics, vol. 5, Butterworth-Heinemann, Oxford, 2003.
[62] S. Chandrasekhar, Stochastic problems in physics and astronomy, Rev. Mod. Phys. 15 (1) (1943).
[63] P. Hänggi, P. Talkner, M. Borkovec, Reaction rate theory: fifty years after Kramers, Rev. Mod. Phys. 62 (2) (1990) 251.
[64] N.G. van Kampen, Stochastic Processes in Physics and Chemistry, second ed., North-Holland, Amsterdam, 2003.
[65] W. Janke, D.A. Johnston, R. Kenna, Phase transition strength through densities of general distributions of zeroes, Nucl. Phys. B 682 (2004) 618.
[66] Mathematica 5.0.1.0, Wolfram Research Inc., ⟨http://www.wolfram.com⟩, 1988–2003.
[67] S. Hilbert, J. Dunkel, Singular microscopic phase transitions in the microcanonical ensemble: an exactly solvable 1*d*-model for evaporation, cond-mat/0511500, 2005.
[68] J.D. Ramshaw, Entropy ambiguity in a system in equilibrium with a finite heat bath, Phys. Lett. A 198 (1995) 122.
[69] P. Chomaz, F. Gulminelli, Generalized definitions of phase transitions, Physica A 305 (2002) 330.
[70] A.B. Adib, A.A. Moreira, J.S. Andrade Jr., M.P. Almeida, Tsallis thermostatistics for finite systems: a Hamiltonian approach, Physica A 322 (2003) 276.
[71] C. Tsallis, Possible generalization of Boltzmann–Gibbs statistics, J. Stat. Phys. 52 (1988) 479.
[72] E.M.F. Curado, C. Tsallis, Generalized statistical mechanics: connection with thermodynamics, J. Phys. A 52 (1991) 479 (corrigenda: 24 (1991) 3187 and 25 (1993) 1019).
[73] D.H.E. Gross, Non-extensive systems follow Boltzmann's principle not Tsallis statistics—phase transitions, second law of thermodynamics, Physica A 305 (2002) 99.